FLOW CHARACTERISTICS OF REAL SHEAR THICKENING FLUIDS THROUGH VARIOUS TYPES OF CHANNELS

GARIMA VISHAL

DEPARTMENT OF CHEMICAL ENGINEERING
INDIAN INSTITUTE OF TECHNOLOGY DELHI
JULY 2025

FLOW CHARACTERISTICS OF REAL SHEAR THICKENING FLUIDS THROUGH VARIOUS TYPES OF CHANNELS

by

GARIMA VISHAL

Department of Chemical Engineering

Submitted

in partial fulfillment of the requirements of the degree of Doctor of Philosophy

to the

INDIAN INSTITUTE OF TECHNOLOGY DELHI

July 2025

Dedicated to Maa, Papa and my son Yuvin

Certificate

This is to certify that the thesis entitled **"Flow characteristics of real shear thickening fluids through various types of channels"**, submitted by **Garima Vishal** to the Indian Institute of Technology Delhi, for the award of the degree of **Doctor of Philosophy** in chemical engineering, is a record of the original, bona fide research work carried out by him under our supervision and guidance. The thesis has reached the standards fulfilling the requirements of the regulations related to the award of the degree.

The results contained in this thesis have not been submitted in part or in full to any other University or Institute for the award of any degree or diploma to the best of our knowledge.

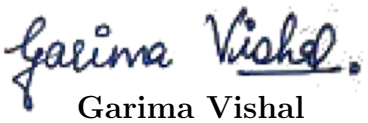

Garima Vishal
Department of Chemical Engineering
Indian Institute of Technology Delhi

Prof. Sudip K Pattnayek
Department of Chemical engineering,
Indian Institute of Technology Delhi.

Prof. Jayati Sarkar
Department of Chemical engineering,
Indian Institute of Technology Delhi.

Acknowledgements

It was a once-in-a-lifetime opportunity that will be an important chapter of my life. There are a number of people without whom this thesis might not have been written and to whom I am greatly indebted for their part in my success. It is a pleasant aspect that I now have the opportunity to express my gratitude for all of them.

First, I would like to express my special thanks of gratitude to my supervisor Prof. Sudip K. Pattanayek, and co-supervisor Prof. Jayati Sarkar. This work would not have been possible without their guidance, support, and encouragement. They have given me full liberty to pursue my research work. Under their guidance, I successfully overcame many difficulties and learned a lot. I am also greatful to Dr. Ashish Garg who has contributed in my research work.

I am also thankful to the Head of the Department of Chemical Engineering Indian Institute of Technology, Delhi. I would also like to thank my thesis committee members and all the faculty members of the Department of Chemical Engineering. I am thankful to all the administrative and technical staff members Department of Chemical Engineering, Indian Institute of Technology, Delhi, for their help and cooperation.

Special gratitude to my respected seniors and juniors Dr. Shalini Shikha, Mr. Deepak, Dr. Mohit, Dr. Prateek Yadav, Mr. Akshat Lohiya, Mr Yogesh, Dr Swati, Mr. Nitin and Mr. Yashwant, for their time-to-time outstanding scientific guidance and for making research work more cordial.

I would like to thank those whom I deeply love, respect, and admire and to whom I dedicate this thesis– my family and my husband Vivek for their help, moral support, and motivation.

At last, thanks to the almighty God who has given me the spiritual support and courage to carry out this work.

Abstract

The rheology of a concentrated mixture of narrowly dispersed silica nanoparticles suspended in a liquid medium having non-Newtonian fluid properties can be described by a combination of shear-thickening fluid (STF), Newtonian, and shear-thinning fluid properties. The fluids with this kind of combined behaviour is termed here as the real shear-thickening fluids. The correlation between shear and viscosity can be effectively modelled using a piecewise approach. Understanding the flow behaviour of real STFs in intricate geometries, particularly within confined spaces, is crucial in developing impact-resistant systems, such as bulletproof vests and protective padding. The understanding of flow characteristics of real STFs through simple geometries like straight channels, converging-diverging channels, and circular surfaces confined in a straight channels are also not reported in the literature. The Lattice Boltzmann method (LBM), a mesoscopic simulation technique is expected to be easier in implementing due to its enhances numerical stability and ease of using various boundary conditions. The no-slip boundary, where the fluid has zero velocity relative to the surface, is commonly assumed in applications. Further investigation compares numerical results with theoretical outcomes for Newtonian and non-Newtonian fluid flow through converging-diverging channels followed by uniform height channels. Significant differences in pressure distribution are observed within the converging-diverging regions, influenced by factors like viscosity and section angles. Higher pressure drops near the throat region lead to elevated shear rates and predominant shear-thickening fluid flow. When flowing over a circular surface, real STFs exhibit a complex wake flow pattern compared to Newtonian and power-law fluids. Thinning behaviour near the centerline results in less intense vortex shedding and recirculation compared to Newtonian flow. Slip conditions gain prominence in microfluidics and nanofluidics where viscosity effects become substantial. The slip at the boundary is implemented through a modified bounce-back and specular reflection (MBSR) scheme in LBM. The theoretical framework deduces interactions between parameters of the combination and the slip length, reliant on specified slip length and relaxation time. These integrated slip boundary conditions are analysed for distinct results. However, due to the challenges of accurately incorporating slippage into models, the effect of slip on the fluid flow behaviour of such materials

has not been extensively studied in literature hence to explore these effects, the slip condition for real STF flow through a straight channel is examined, with numerical outcomes compared to analytical results for fluid flow featuring a combination of shear-thickening and shear-thinning behaviours, each characterized by distinct power-law indices. Results indicate that at low shear rates, Newtonian flow dominates, transitioning to shear-thinning and then shear-thickening as the shear rate increases.

Keywords:
Shear-thickening fluid, Non-Newtonian fluid, Lattice Boltzmann method, Channel flow, Converging-diverging channel, Theoretical model

सारांश

संकीर्ण रूप से वितरित सिलिका नैनोकणों के एक सघन मिश्रण की रियोलॉजी, जो एक गैर-न्यूटोनियन तरल माध्यम में निलंबित होते हैं, को शीयर-थिकनिंग फ्लूड (STF), न्यूटोनियन और शीयर-थिनिंग फ्लूड गुणों के संयोजन के रूप में वर्णित किया जा सकता है। इस प्रकार के सम्मिलित व्यवहार वाले तरलों को यहाँ "वास्तविक शीयर-थिकनिंग फ्लूड्स" कहा गया है। शीयर और विस्कोसिटी के बीच सहसंबंध को प्रभावी रूप से एक पीसवाइज़ (खंडानुसार) दृष्टिकोण का उपयोग करके मॉडल किया जा सकता है। वास्तविक STF के प्रवाह व्यवहार को जटिल ज्यामितियों में, विशेष रूप से संकीर्ण स्थानों में, समझना अत्यंत महत्वपूर्ण है जैसे कि बुलेटप्रूफ जैकेट्स और सुरक्षात्मक पैडिंग जैसी प्रभाव-प्रतिरोधी प्रणालियों के विकास में।

सरल ज्यामितियों जैसे सीधे चैनल, संकीर्ण-फैलते हुए चैनल और सीधे चैनलों में सीमित वृत्तीय सतहों के माध्यम से वास्तविक STF के प्रवाह लक्षणों को समझने का कार्य अभी तक साहित्य में रिपोर्ट नहीं किया गया है। लैटिस बोल्ट्ज़मैन विधि (LBM), एक मेसोस्कोपिक सिमुलेशन तकनीक है, जिसे विभिन्न सीमा स्थितियों के उपयोग में आसानी और बढ़ी हुई संख्यात्मक स्थिरता के कारण लागू करना अपेक्षाकृत सरल माना जाता है। अनुप्रयोगों में आमतौर पर नो-स्लिप सीमा की धारणा ली जाती है, जहाँ तरल की गति सतह के सापेक्ष शून्य होती है।

इसके बाद के अध्ययन में न्यूटोनियन और गैर-न्यूटोनियन तरल प्रवाह के लिए सैद्धांतिक परिणामों की तुलना संकुचित-फैलते हुए चैनलों और उसके बाद के समान ऊँचाई वाले चैनलों में की गई है। संकुचित-फैलते हुए क्षेत्रों में दबाव वितरण में महत्वपूर्ण अंतर पाए गए हैं, जो विस्कोसिटी और अनुभाग कोण जैसे कारकों से प्रभावित होते हैं। थ्रोट क्षेत्र के पास उच्च दबाव हानि के कारण उच्च शीयर दर उत्पन्न होती है, जिससे प्रमुख रूप से शीयर-थिकनिंग प्रवाह होता है।

जब एक वृत्तीय सतह के ऊपर प्रवाह होता है, तो वास्तविक STF न्यूटोनियन और पावर-लॉ तरलों की तुलना में एक जटिल वेक फ्लो पैटर्न प्रदर्शित करते हैं। केंद्र रेखा के पास थिनिंग व्यवहार के कारण, न्यूटोनियन प्रवाह की तुलना में कम तीव्र वोर्टेक्स शेडिंग और पुनः परिसंचरण होता है। माइक्रोफ्लूडिक्स और नैनोफ्लूडिक्स में, जहाँ विस्कोसिटी प्रभाव महत्वपूर्ण हो जाते हैं, स्लिप स्थितियाँ अधिक महत्त्वपूर्ण हो जाती हैं। LBM में स्लिप को एक संशोधित बाउंस-बैक और स्पेक्युलर रिफ्लेक्शन (MBSR) योजना के माध्यम से लागू किया गया है।

सैद्धांतिक ढाँचे में संयोजन के मानदंडों और स्लिप लंबाई के बीच की परस्पर क्रियाओं को स्पष्ट किया गया है, जो निर्दिष्ट स्लिप लंबाई और विश्राम समय पर आधारित होती हैं। इन एकीकृत स्लिप सीमा स्थितियों का विशिष्ट परिणामों के लिए विश्लेषण किया गया है। हालाँकि, मॉडलों में स्लिप को सटीक रूप से शामिल करना चुनौतीपूर्ण होने के कारण, ऐसे पदार्थों के तरल प्रवाह व्यवहार पर स्लिप के प्रभाव का अध्ययन साहित्य में व्यापक रूप से नहीं किया गया है। इसलिए इन प्रभावों का पता लगाने के लिए, एक सीधे चैनल में वास्तविक STF प्रवाह के लिए स्लिप स्थिति की जाँच की गई है, और संख्यात्मक परिणामों की तुलना विश्लेषणात्मक परिणामों से की गई है, जिसमें शीयर-थिकनिंग और शीयर-थिनिंग व्यवहारों के संयोजन की विशेषता वाले तरल प्रवाह शामिल हैं, प्रत्येक को विशिष्ट पावर-लॉ सूचकांकों द्वारा दर्शाया गया है। परिणाम दर्शाते हैं कि कम शीयर दरों पर न्यूटोनियन प्रवाह प्रभावी होता है, जो कि शीयर-थिनिंग और फिर उच्च शीयर दर पर शीयर-थिकनिंग में परिवर्तित हो जाता है।

कीवर्ड्स:

शीयर-थिकनिंग फ्लूड, गैर-न्यूटोनियन फ्लूड, लैटिस बोल्ट्ज़मैन विधि, चैनल प्रवाह, संकुचित-फैलते हुए चैनल, सैद्धांतिक मॉडल

Contents

Certificate

Acknowledgements

Abstract

Contents

List of Figures

List of Tables

1 Introduction **1**
1.1 Objectives 6

2 Literature Review **11**
2.1 Jamming of fluids during their operation 12
2.2 STF in various applications 12
2.2.1 Body armor and protective Gear 13
2.2.2 Sports and impact protection 14
2.2.3 Automotive Safety: 15
2.2.4 Industrial gloves 16
2.2.5 Damping and vibration control: 16
2.2.6 Footwear: 17
2.2.7 Robotics 17
2.2.8 Orthopedic devices 18
2.2.9 Application of STF in batteries 19
2.2.10 Civil engineering and infrastructure 19
2.3 Fluids and their classification 20
2.3.1 Power-Law Model 21

2.3.2 Carreau mode . . . 23
2.3.3 Real Shear thickening fluid (STF) . . . 24
2.4 Length scale and simulation technique . . . 25
2.5 Flow of various fluids through various geometries . . . 27
2.5.1 Flow of fluids through straight channels . . . 29
2.5.1.1 Flow of Newtonian fluids through strainght channels 30
2.5.1.2 Flow of non-Newtonian power law fluid . . . 31
2.5.1.3 Flow of shear thinning fluid through channel . . . 32
2.5.1.4 Flow of shear thickening fluid through channels . . . 33
2.5.1.5 Slip condition in channel flow . . . 34
2.5.2 Flow of fluids through converging-diverging channels . . . 37
2.5.3 Flow of fluids over curved surface . . . 41
2.6 The Lattice Boltzmann Equation and BGK Approximation . . . 44
2.6.1 BGK Approximation . . . 45
2.6.2 Discretization: Lattice Boltzmann Equation . . . 45
2.6.3 Discrete Velocity Set . . . 46
2.6.4 Discrete Distribution Functions . . . 46
2.6.5 Discrete Equilibrium Distribution . . . 46
2.6.6 Lattice Boltzmann Equation . . . 47
2.6.7 Chapman-Enskog Expansion . . . 47
2.6.8 Multiscale Expansion . . . 47
2.6.9 Zeroth-Order Approximation . . . 47
2.6.10 First-Order Approximation . . . 48
2.6.11 Second-Order Approximation . . . 48
2.6.12 Macroscopic Variables . . . 48
2.6.13 Derivation of Continuity Equation . . . 49
2.6.14 Derivation of Navier-Stokes Equation . . . 49
2.6.15 Left Side Simplification . . . 49
2.6.16 Right Side Simplification . . . 50
2.6.17 Combining Terms . . . 50
2.7 Research Gaps . . . 53
2.8 Conclusion . . . 53

3 The channel flow of a real shear thickening fluid using the Lattice Boltzmann Simulation and the Theoretical Model 73
3.1 Introduction . . . 74
3.2 Model Description: . . . 76
3.2.1 Numerical method . . . 77
3.2.2 Non Newtonian 2D fluid model . . . 79
3.2.3 Boundary condition (BC) . . . 80
3.2.3.1 Bounce back boundary condition . . . 81
3.2.3.2 Velocity - Pressure boundary condition . . . 81

3.3 Analytical Model for two-phase and three-phase mimicking real STF viscosity . . . 83
3.3.1 Three-phase mimicking real STF viscosity model . . . 83
3.3.1.1 Governing equations (Cauchy equations) . . . 83
3.3.1.2 Boundary conditions . . . 84
3.3.2 The Theoretical Model . . . 85
3.3.2.1 Mimicking real STF viscosity model . . . 85
3.3.2.2 2D planar model . . . 86
3.3.2.3 In region I: $\eta = \eta_I$ for $0 \leq z \leq z_1$ . . . 87
3.3.2.4 In region II: $\eta = \eta_{II}$ for $z_1 \leq z \leq z_2$ . . . 88
3.3.2.5 In region III: $\eta = \eta_{III}$ for $z_2 \leq z \leq H/2$ . . . 89
3.3.2.6 Calculation of c_1, c_2, and c_3 . . . 89
3.3.2.7 Two-phase viscosity model . . . 90
3.3.3 Parameters used in LBM and in the theoretical model . . . 90
3.4 Results and discussion . . . 92
3.5 Conclusions . . . 104

4 Real Shear Thickening Fluid (STF) Flow in Converging-Diverging Channels: Analytical and Lattice Boltzmann Study 113
4.1 Introduction . . . 114
4.2 System Description . . . 116
4.3 Lattice Boltzmann Method . . . 118
4.4 Governing equations and Boundary conditions . . . 121
4.4.1 Governing (Cauchy) equations . . . 122
4.4.2 Boundary conditions . . . 122
4.5 The Theoretical Model . . . 123
4.5.1 2D planar model . . . 123
4.5.2 Newtonian fluid flow in conical channel . . . 124
4.5.3 Power-law fluid flow in conical channel . . . 126
4.5.4 Two phase viscosity fluid flow in conical channel . . . 128
4.5.4.1 In region I: $\eta = \eta_{II}$ for $0 \leq x_2 \leq z_1$ . . . 128
4.5.4.2 In region II: $\eta = \eta_{II}$ for $z_1 \leq x_2 \leq H(x_1)/2$ . . . 129
4.5.4.3 Calculation of c_4, and c_5 . . . 129
4.6 Results and discussions . . . 130
4.6.1 Newtonian fluid flow at different conical angle θ . . . 130
4.6.2 Newtonian fluid flow at different magnitude of viscosity η . . . 133
4.6.3 Shear-thinning fluid ($\eta = 0.03(\dot{\gamma})^{0.7-1}$) flow at different conical angle θ . . . 135
4.6.4 Shear-thickening fluid ($\eta = 2.8(\dot{\gamma})^{1.4-1}$) flow at different conical angle θ . . . 139
4.6.5 Shear-thinning and thickening two phase fluid flow . . . 144
4.7 Conclusions . . . 147

5 Modelling of Real Shear Thickening Fluid (STF) Flow around a Circular Cylinder within a Channel using the Lattice Boltzmann Method **155**
5.1 Introduction . . . 156
5.2 Model Description . . . 158
5.2.1 Boundary Conditions : . . . 159
5.3 Results and discussions . . . 163
5.3.1 Newtonian fluid Flow . . . 164
5.3.2 Shear-thinning fluid Flow . . . 166
5.3.3 Shear-thickening fluid Flow . . . 168
5.3.4 Real Shear-thickening fluid Flow . . . 170
5.3.5 Comparison of velocity profiles of the above fluid flows at various axial locations . . . 172
5.3.6 Comparison of coefficient of pressure (C_p) on the surface of the cylinder for the above mentioned fluid flows . . . 174
5.4 Conclusions . . . 176

6 The effect of slip boundary on the flow characteristics of real shear thickening fluids through channel **183**
6.1 Introduction . . . 184
6.2 Numerical method . . . 186
6.2.1 Boundary conditions . . . 187
6.3 Model Description . . . 190
6.4 Theoretical Model with slips for mimicking real STF viscosity . . . 190
6.4.1 Three-phase mimicking real STF viscosity model with slip effects 190
6.4.1.1 Governing equations (Cauchy equations) . . . 191
6.4.1.2 Boundary conditions . . . 191
6.4.2 The Theoretical Model . . . 192
6.4.2.1 Mimicking real STF viscosity model . . . 192
6.4.2.2 2D planar model . . . 192
6.4.2.3 In region I: $\eta = \eta_I$ for $0 \leq z \leq z_1$ . . . 193
6.4.2.4 In region II: $\eta = \eta_{II}$ for $z_1 \leq z \leq z_2$ . . . 194
6.4.2.5 In region III: $\eta = \eta_{III}$ for $z_2 \leq z \leq H/2$ . . . 195
6.4.2.6 Calculation of c_1, c_2, and c_3 . . . 195
6.5 Results and Discussion . . . 196
6.5.1 Effect of varying pressure on flow characteristics of real STF viscosity fluid . . . 202
6.5.2 Effect of varying channel's height on flow characteristics of real STF viscosity fluid . . . 205
6.6 Conclusion . . . 207

7 Conclusion **213**

7.1 Flow through a straight channel with no-slip condition 214
7.2 Flow through a converging-diverging channel with no-slip condition . 215
7.3 Flow over circular surface confined in a channel with no-slip condition 216
7.4 Flow through a straight channel with slip condition 217
7.5 Future Scope of Work 217
7.6 Conferences attended 219
7.7 List of publication 219

Scope for Future Work **220**

List of Figures

1.1 Schematics of a high tensity fabric soaked in a Shear Thickening Fluids. . . . 2
1.2 Schematics of variation of Viscous Behaviour of an STF under varying shear rate. The inset figures show the schematics of particle arrangements at different conditions. . . . 4

2.1 Fabriction of body armor using STF treated yarns 14
2.2 STF impregnated industrial gloves. . . . 16
2.3 STF treated footwear for sports and orthopedic purpose. . . . 17
2.4 schematic diagram of types of fluid 21
2.5 Viscosity vs strain rate variation non newtonian fluids 22
2.6 Different length scales and geometries of the system. . . . 27
2.7 Velocity profiles for no slip and slip boundary conditions. . . . 30
2.8 Velocity profile for different fluids with constant mass flow inlet . . . 33
2.9 Velocity profiles for no slip and slip boundary conditions. . . . 35
2.10 Different boundary conditions for slip length (λ). . . . 35

3.1 Schematics of various aspects of system of our interest using LBM (A) Schematic diagram of the flow geometry. (B) The rectangular grid discretization for the LBM analysis and (C) the D2Q9 velocity model used in LBM to solve the flow problem 76
3.2 Bounce back and velocity-pressure boundary condition depictions using the distribution function 82
3.3 Schematic diagram of the upper half part of the shallow channel of length L, cross–sectional width W, and height H. The Cartesian axis is taken at the mid plane of the channel. . . . 83
3.4 The relation between strain rate and viscosity for real shear thickening fluid. . . . 85
3.5 Velocity profile of power-law fluids at different locations of the channel. A(n=0.7, m=0.05) and B: (n=1.4, m=0.05). . . . 93
3.6 Comparison of various flow characteristics as obtained by simulation (at the fully developed region) and analytical calculation (A) Velocity (B) Strain rate (C) Viscosity. . . . 94

3.7 Variation of friction factor with the Reynolds number for different power-law index and m=0.05. Solid line compares the analytical calculation 95
3.8 Effect of change over viscosity for the flow of the fluid with stress-dependent viscosity. Selected stress cutoffs are 1.77 x 10^{-5} Fu/lu^2, 2.33 x 10^{-5} Fu/lu^2 and 3.03 x 10^{-5} Fu/lu^2 for the case n_1=0.7, m_1=0.03 and n_2=0.9, m_2=0.05: Comparision of profiles for simulation results (A) Velocity profile (B) Pressure Vs Flow rate 96
3.9 Effect of change over viscosity for the flow of the fluid with stress-dependent viscosity. Selected stress cutoffs are $\tau_1 = 3.72$ x 10^{-6} Fu/lu^2 , τ_2 = 4.9 x 10^{-6} Fu/lu^2 and τ_3 = 6.28 x 10^{-6} Fu/lu^2 for the case n1=0.9, m1=0.03 and n2=1.1, m2=0.05: Comparision of profiles for simulation results (A) Velocity profile (B) Pressure Vs Flow rate . . . 97
3.10 The flow characteristics of a real shear thickening fluid 99
3.11 The real mimicked STF viscosity in (a) how flow rate in the upper half of the channel per unit width varies as a function of pressure and in (b) the region height varies as a function of pressure. Here, Q1, Q2, and Q3 are the flow rates in regions 1 (Newtonian core), 2 (shear thinning intermediate), and 3 (shear thickening near channel wall), respectively. 101
3.12 The real mimicked STF viscosity in (a) how flow rate in the upper half of the channel per unit width varies as a function of pressure and in (b) the region height varies as a function of pressure. Here, Q1, Q2, and Q3 are the flow rates in regions 1 (Newtonian core), 2 (shear thinning intermediate), and 3 (shear thickening near channel wall), respectively. 101
3.13 For the given real shear thickening fluid viscosity graphs show (a) how the flow rate in the upper half of the channel per unit width varies as a function of the channel's height. Here, Q1, Q2, and Q3 are the flow rates in regions 1 (Newtonian core), 2 (shear thinning intermediate), and 3 (shear thickening near channel wall), respectively. 102

4.1 Schematic diagram showing geometric parameters for the flow of fluid through the converging- diverging section. 117
4.2 D2Q9 model for Lattice Boltzmann method with the boundary for a node (a) inside and on the wall (b) a converging and diverging wall boundary 118
4.3 Comparison of Lattice Boltzmann Simulation (LBM) results with the theoretical predictions for the pressure along the centreline of the channel for different angles at constant viscosity of $\eta = 0.4$ 132
4.4 Velocity contour plot of Newtonian fluid ($\eta = 0.4$) at angles (a) 11.3^o , (b) 14.03^o , (c) 16.7^o 133

4.5 Comparison of Lattice Boltzmann Simulation (LBM) results with the theoretical predictions for the pressure along the centreline of the channel for different Newtonian viscosities at given $\theta = 14.03^o$ 134
4.6 Velocity contour plot for different viscosities of Newtonian fluid (a) 2.8, (b) 0.4, (c) 0.03.. 135
4.7 Comparison of Lattice Boltzmann Simulation (LBM) results with the theoretical predictions for the pressure along the centreline of the channel for shear thinning fluid flow at varying θ: 11.3^o, 14.03^o, and 16.7^o, respectively. 136
4.8 Contour plot of velocity for Shear-thinning fluid for viscosity consistency index 0.03 and power index= 0.7 at angles (a) 11.3°, (b) 14.03°, (c) 16.7° 137
4.9 Contour plot of strain rate for Shear-thinning fluid for viscosity consistency index 0.03 and power index= 0.7 at angles (a) 11.3°, (b) 14.03°, (c) 16.7° 138
4.10 Contour plot of viscosity for Shear-thinning fluid for viscosity consistency index 0.03 and power index= 0.7 at angles (a) 11.3°, (b) 14.03°, (c) 16.7° 139
4.11 Comparison of Lattice Boltzmann Simulation (LBM) results with the theoretical predictions for the pressure along the centreline of the channel for shear thickening fluid flow at varying θ: 11.3^o, 14.03^o, and 16.7^o, respectively. 140
4.12 Contour plot of velocity for Shear-thickening fluid for viscosity consistency index 2.8 and power index= 1.4 at angles (a) 11.3°, (b) 14.03°, (c) 16.7° 141
4.13 Contour plot of strain rate for Shear-thickening fluid for viscosity consistency index 2.8 and power index= 1.4 at angles (a) 11.3°, (b) 14.03°, (c) 16.7° 142
4.14 Contour plot of viscosity for Shear-thickening fluid for viscosity consistency index 2.8 and power index= 1.4 at angles (a) 11.3°, (b) 14.03°, (c) 16.7° 143
4.15 Pressure profile for shear thinning(n=0.7,m=0.1, n=1,m=0.6 and n=1.8,m=5.6 144
4.16 Comparison of velocity profiles predictions from the LBM and the theoretical model at varying axial location for given flow rate and density at the inlet at given $\theta = 14.03^o$ 145
4.17 Contours for the case (a) Velocity Contour, (b) Viscosity Contour, (c) Strain rate, (d) Pressure. 146

5.1 Schematic diagram of the domain. 159
5.2 Distribution functions at boundaries (A) Inlet and outlet (B) wall of the cylinder (C) wall of the channel. 160

5.3 Contour plots for Newtonian fluid (a) Velocity contour (b) Pressure contour. 165
5.4 Contour plots for non-Newtonian fluid given case (i) ($n = 0.7$, $m = 0.07$) and case (ii) ($n = 0.7$, $m = 0.06$) (a) Velocity contour (b) Pressure contour (c) Viscosity contour 167
5.5 Contour plots for non-Newtonian fluid given case (i) ($n = 1.4$, $m = 0.17$) and case (ii) ($n = 1.4$, $m = 0.16$) (a) Velocity contour (b) Pressure contour (c) Viscosity contour 168
5.6 Contour plots for non-Newtonian fluid given case ($n_1 = 0.9$, $m_1 = 0.8$) and ($n_2 = 1.2$, $m_2 = 2.8$) (a) Velocity contour (b) Pressure contour (c) Viscosity contour 170
5.7 Contour plots for non-Newtonian fluid given case (a) Velocity contour (b) Pressure contour (c) Viscosity contour 171
5.8 Velocity profiles at various axial locations for (a) Newtonian fluid flow, (b) shear thinning, (c) shear thickening, and (d) real shear thickening fluids, respectively. 172
5.9 Comparison of pressure distribution on the circular cylinder due to Newtonian, Shear thinning, Shear thickening fluid flow using LBM studies, and the literature 174

6.1 The distribution functions for (a) bounce back boundary condition (b) specular bounce back boundary condition 188
6.2 Schematic diagram of the upper half part of the shallow channel of length L, cross–sectional width W, and height H. The Cartesian axis is taken at the mid plane of the channel. 190
6.3 Slip and no slip boundary condition comparison of Newtonian fluid (A) Velocity profile (B) Strain rate profile. 198
6.4 Slip and no slip boundary condition comparison of non-Newtonian fluid (n=0.8,m=0.05) (A) Velocity profile (B) Strain rate vs viscosity profile. 199
6.5 Slip and no slip boundary condition comparison of non-Newtonian fluid (n=1.4, m=0.05) (A) Velocity profile (B) Strain rate vs viscosity profile. 199
6.6 The correlation between strain rate and viscosity in a real shear-thickening fluid is depicted in the plot. The experimental parameters of the real shear-thickening fluid are represented by black circles, while the model fit, derived using equation (3.37), is illustrated by the red line. The analysis reveals three distinct regimes: starting from Newtonian behavior at initial shear rates, transitioning to shear-thinning behavior at moderate shear rates, and finally entering the thickening regime at higher applied shear rates. 200
6.7 The flow characteristics of a real shear thickening fluid at various slip length of (a) $\lambda = 0$ lu, (b) $\lambda = 1$ lu, and (c) $\lambda = 5$ lu, respectively. . 201

6.8 The comparison of magnitude of velocities as a effect of the slip-length for the same flow rate Q 203
6.9 The real mimicked STF viscosity in (a) how flow rate in the upper half of the channel per unit width varies as a function of pressure and in (b) the region height varies as a function of pressure. Here, $Q1, Q2$, and $Q3$ are the flow rates in regions 1 (Newtonian core), 2 (shear thinning intermediate), and 3 (shear thickening near channel wall), respectively. The symbols and the solid lines of the same color show the flow rates and the region height for slip length $\lambda = 0$ lu and 5 lu, respectively. 204
6.10 The real mimicked STF viscosity in (a) how flow rate in the upper half of the channel per unit width varies as a function of pressure and in (b) the region height varies as a function of pressure. Here, $Q1$, $Q2$, and $Q3$ are the flow rates in regions 1 (Newtonian core), 2 (shear thinning intermediate), and 3 (shear thickening near channel wall), respectively. The symbols and the dashed lines of the same color show the flow rates and the region height for slip length $\lambda = 0$ lu and 5 lu, respectively. 205
6.11 For the given real shear thickening fluid viscosity, graphs show (a) how the flow rate in the upper half of the channel per unit width varies as a function of the channel's height. Here, $Q1, Q2$, and $Q3$ are the flow rates in regions 1 (Newtonian core), 2 (shear thinning intermediate), and 3 (shear thickening near channel wall), respectively. The symbols and the dashed lines of the same color show the flow rates and the region height for slip length $\lambda = 0$ lu and 5 lu, respectively. 206

List of Tables

2.1 Comparison of LBM and CFD in Modelling and Simulation 28
2.2 Studies of various fluids flowing through various geometries using LBM only 52

3.1 Model Parameters and Justification for STF Flow Simulations 103

4.1 Details of simulation tests at different conical angles using Newtonian viscosity 131
4.2 Details of simulation tests at different magnitude of viscosity 134
4.3 Details of simulation tests for the shear-thinning fluid flow 135
4.4 Details of simulation tests for the shear-thickening fluid flow 139
4.5 Details of simulation tests for comparing the pressure profile for newtonian and non newtonian fluids at a given Reynolds number 142
4.6 Comparison of Theoretical Method and LBM for STF Flow Modelling 147

5.1 Comparison of drag coefficient values for steady power-law fluid flow over a cylinder for Reynolds number 40 and $\beta = H/d = 4$ 163
5.2 Defining the case study with the symbol (i) and (ii) form different viscosity $\eta = m|\dot{\gamma}|^{n-1}$ 164
5.3 Defining the case study with the symbol (i) and (ii) form different viscosity. Case (i): $n = 0.7, m = 0.07$, Case (ii): $n = 0.7, m = 0.06$ . . 166
5.4 Defining the case study with the symbol A and B form different viscosity. Case (i): $n = 1.4, m = 0.17$, Case (ii): $n = 1.4, m = 0.16$ 169